The Effect of Microstructure on Fatigue Crack Initiation in Ti-6Al-4V

A.L. Pilchak[1], *A. Bhattacharjee*[1], *R.E.A. Williams*[1], *J.C. Williams*[1]
[1]*The Ohio State University, Columbus, USA*

The role of microstructure, including constituent morphology, microtexture and local crystallographic orientation, on fatigue crack initiation in Ti-6Al-4V has been investigated. Four point bend fatigue tests have been performed on samples with equiaxed, bi-modal, fully lamellar and bi-lamellar microstructures. The fractured specimens have been characterized using quantitative fractography and electron backscatter diffraction. The results are discussed on the basis of slip length, slip planarity and local crystallographic orientation.

1.0 Introduction

The microstructure and, therefore, the mechanical properties of α + β titanium (Ti) alloys can be tailored for specific applications by carefully choosing a sequence of thermomechanical processes and heat treatments to obtain certain morphologies and spatial distributions of the α phase. Two morphologies are prevalent in Ti alloys, namely, equiaxed and lamellar. Certain processing routes [1] can result in a material with a bi-modal microstructure, containing both equiaxed and lamellar α phase. While both equiaxed and bi-modal microstructures appear fully recrystallized when investigated by optical and scanning electron microscopy, electron backscatter diffraction (EBSD) analysis has revealed that the grains can share common c-axis orientation over length scales of hundreds of microns. The boundaries between the aptly name microtextured regions has been implicated in dwell fatigue failures in the near α alloy Ti-6242 [2,3].

In Ti alloys, high cycle fatigue strength scales well with yield strength [1,4], both increasing with decreasing constituent length scale. The absence of hard second phases and inclusions, which are typical crack initiation sites in steels, drives crack initiation to the next 'weakest link', which is usually a slip band [5-7]. As will be discussed, slip length and slip planarity are the two most important factors which influence the fatigue properties of Ti alloys [1,6,7]. To a first approximation, slip length is governed by the distance that a dislocation could travel within a region of constant crystallographic orientation without encountering an interface. Slip length can be controlled by microstructural features including α laths, α/α boundaries, phase boundaries and colony boundaries. The limiting feature is microstructure specific, however, because slip bands can cross morphological barriers if the adjacent constituents have similar crystal structure. The second important factor, slip planarity, tends to increase with increasing oxygen and aluminum content [8,9], and also when α_2 (Ti_3Al) is precipitated within the α phase [1,9]. The α_2 phase has an ordered DO_{19} structure which strengthens the α phase by providing a barrier to dislocation motion, but results in strain localization if the coherent α_2 particles are sheared [9].

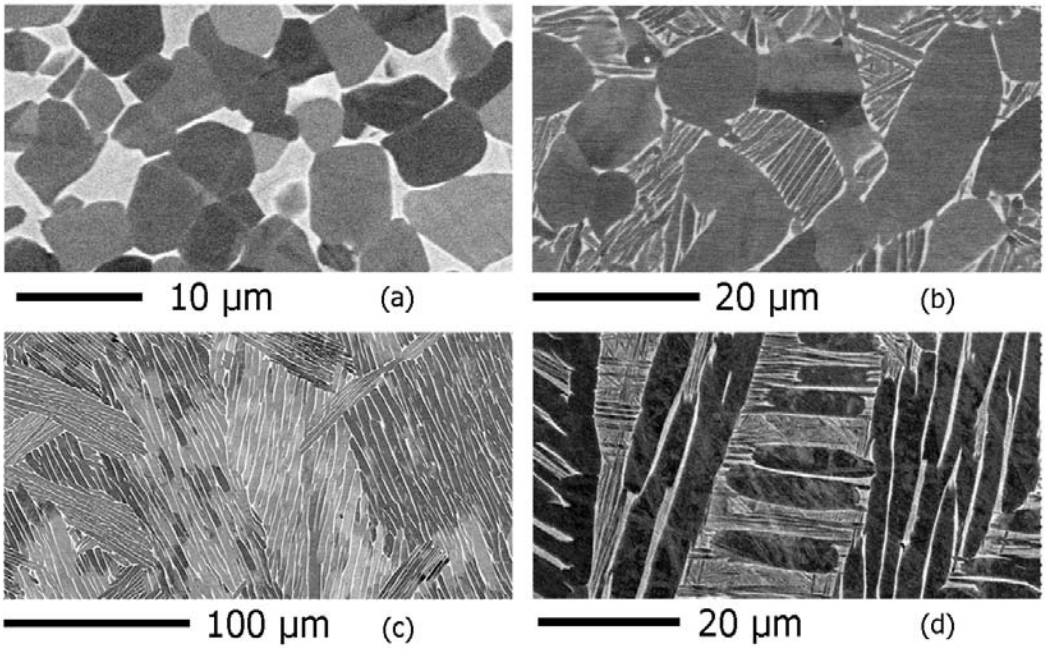

Figure 1. Backscattered electron micrographs of the materials investigated in the present study. (a) equiaxed, (b) bi-modal, (c) fully lamellar and (d) bi-lamellar.

2.0 Experimental approach, materials and methods

While Ti-6-4 is the most widely used Ti alloy for structural components, there is little fundamental understanding of the effect of local microstructure on fatigue crack initiation. Therefore, in the present study, we have performed four point bend fatigue tests on Ti-6-4 with a range of microstructures and characterized the crack initiation sites using electron backscatter diffraction to obtain local crystallographic orientation.

In the mid 1970's, a program was initiated to study the influence of metallurgical factors including microstructure and interstitial content on mechanical properties, including fatigue crack growth (FCG), of Ti-6-4 and Ti-6246 over a range of microstructures [4]. In the present study, we have extracted four point bend specimens from the remaining halves of the compact tension (CT) specimens of Ti-6-4 used in the earlier study [4]. The oxygen and iron contents of the starting billet of Ti-6-4 were 0.122 and 0.22 wt pct., respectively. In addition to wrought material extracted from the CT's, cast and hot isostatically pressed Ti-6-4 with an oxygen content of 0.19 wt pct. was investigated in the fully lamellar and bi-lamellar conditions. Due to space limitations, we have selected a subset of data for presentation here consisting of equiaxed, bi-modal, fully lamellar and bi-lamellar microstructures (Fig. 1). A more complete characterization of these microstructural conditions can be found in the report [4], but here we provide brief descriptions of the four conditions selected for this study as this is necessary to understand our results.

The equiaxed condition (Fig. 1a) contained α grains with an average grain diameter of 15 μm. The volume fraction of α was 89 pct. which was balanced by β phase located primarily at α triple points. The larger β regions often contained a fine scale β transformation product. Despite the fully recrystallized appearance when imaged optically, the TEM investigations [4] revealed the presence of low angle boundaries between the equiaxed α grains. EBSD analyses showed that these networks of low angle boundaries extended over several hundred microns consistent with the presence of substantial microtexture in these samples.

The bi-modal (Fig. 1b) condition differed from the equiaxed material only by final heat treatment [4]. There was, by volume, approximately 50 pct. equiaxed α balanced by colony α + β. Both the equiaxed α grain diameter and the α colony size was approximately 15 μm. Due to variant selection, the c-axes in the majority of the α + β colonies were nearly parallel to the c-axes in nearby equiaxed α grains. As a result, the size of the microtextured regions was similar in the equiaxed and bi-modal conditions. However, within the microtextured regions there were infrequent observation of grains and colonies with angles of 60^o or 90^o between their basal poles.

The cast and hot isostatically pressed material (Fig. 1c) contained a coarse, fully lamellar microstructure. The prior β grain size was on the order of 1 mm with α colonies ranging from 100 μm to 500 μm. The α laths were approximately 3 to 5 μm thick depending on which two dimensional section of the three dimensional lath was coincident with the plane of polish. The narrower dimension was observed when [0001] and $[2\bar{1}\bar{1}0]$ were nearly normal to the plane of polish. No α precipitates were observed in the parent β phase remaining between the laths.

The bi-lamellar microstructure (Fig 1d) was obtained by heat treating the fully lamellar material in the α+β phase field at 970 ^{o}C for 2 hours followed by air cooling. This heat treatment increased the volume fraction of β phase between the α laths which then decomposed to form fine secondary α in the interlamellar β phase upon cooling.

Constant amplitude four point bend fatigue tests were conducted at a frequency of 60 Hz and a load ratio of 0.1. At least six fatigue tests were conducted for each condition; the maximum stress levels are reported below for each condition. The surfaces of the four point bend specimens were polished through 0.05 μm colloidal silica suspension prior to testing. Careful preparation of the fatigue specimens has been found to be critical to avoid corner crack initiation. Further details of the sample preparation and testing have been described elsewhere [10]. One half of each fractured specimen was examined in a scanning electron microscope (SEM). The fatigue crack initiation sites were identified by locating the faceted features on the fracture surface which are typical at short crack lengths [11]. Quantitative tilt fractography [12,13] was used in conjunction with the orientations obtained by EBSD to accurately determine the fracture plane of individual grains.

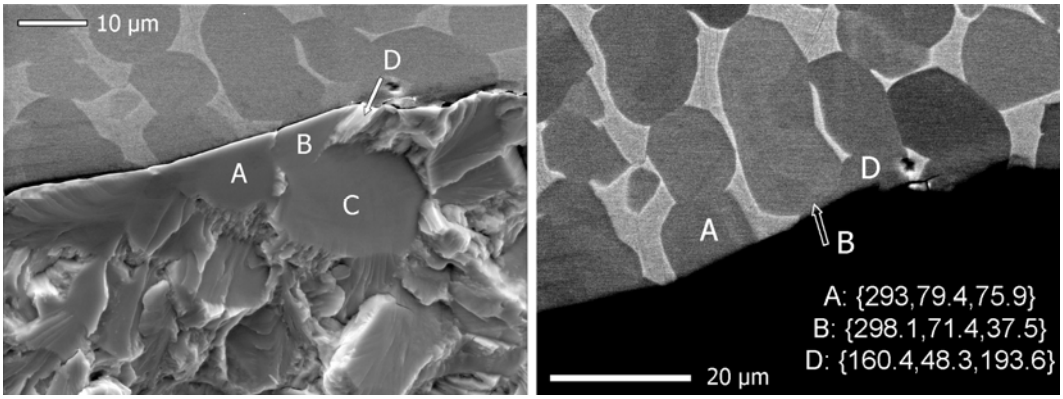

Figure 2. Crack initiation site and the surrounding microstructure of the equiaxed microstructure. Max stress: 636 MPa, Cycles to failure (N_f) = 74,593.

3.0 Results and discussions

Presentation of EBSD data in black and white media poses a challenge. To overcome this issue, we show backscattered electron images with orientations numerically assigned as Euler angles following Bunge's convention [14]. The sample reference frame was defined by three mutually perpendicular vectors $x1$, $x2$ and $x3$ parallel, respectively, to the long, short transverse and thickness directions of the four point bend specimens. Bunge describes a crystal orientation using three angles $\{\varphi_1, \Phi, \varphi_2\}$ that describe three successive rotations about the c_3, c_1 and c_3 axes of the crystal basis. These rotations can be thought of as those necessary to bring the basis of the sample reference frame into coincidence with that of the crystal reference frame. The crystal axes were attached to the sample reference frame with the convention described by Nye [15] where $c_1 \parallel [2\bar{1}\bar{1}0] \parallel x1$ and $c_3 \parallel [0001] \parallel x3$ at $\{0, 0, 0\}$. So, for example, the orientation $\{0, 90, 30\}$ is reached by making a rotation of 90^o about c_1 so $[0001]$ becomes parallel to $x2$ and $c_1 \parallel [2\bar{1}\bar{1}0]$ remains parallel to $x1$. Then, a 30^o rotation about the newly oriented crystal $[0001]$ axis results in $[1\bar{1}00]$ becoming parallel to $x1$. We have assumed that the stress field in the vicinity of the small surface cracks can be approximated by uniaxial tension. It is recognized that the grain level stress state is actually orientation dependent and not necessarily uniaxial [16], but a simplified analysis is used here to show trends.

We briefly summarize the fracture surface observations applicable to all of the microstructural conditions. First, crack initiation was not the result of a classical slip band intrusion/extrusion mechanism at the surface [17]. Instead, crack initiation typically occurred within a grain diameter of the polished surface at a grain boundary. This is consistent with the observation of Baxter et al. [18] who performed four point bend fatigue tests on IMI-834 with a bi-modal microstructure and observed near, but sub-surface initiation. Second, the crack initiation sites all contained planar facets that were comparable in size to the length scale of the underlying microstructural constituents. Our recent work has

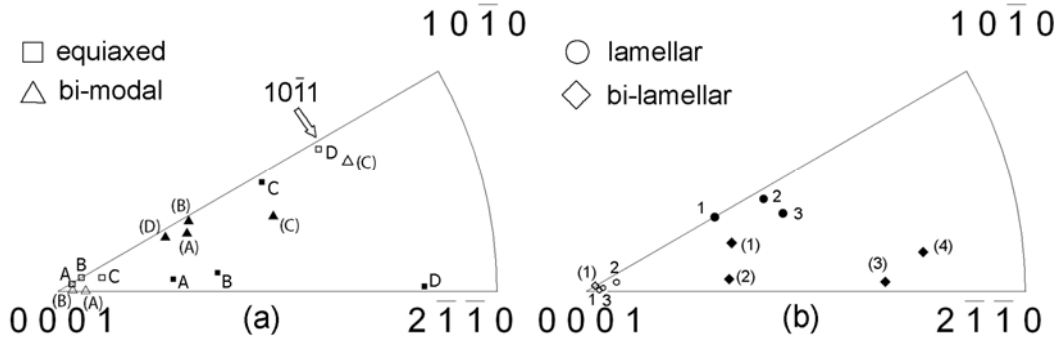

Figure 3. Equal angle projections showing crystal orientations relative to the loading direction (filled symbols) and the facet normal (open circles) when available for (a) the equiaxed and bi-modal conditions and (b) the lamellar and bi-lamellar conditions.

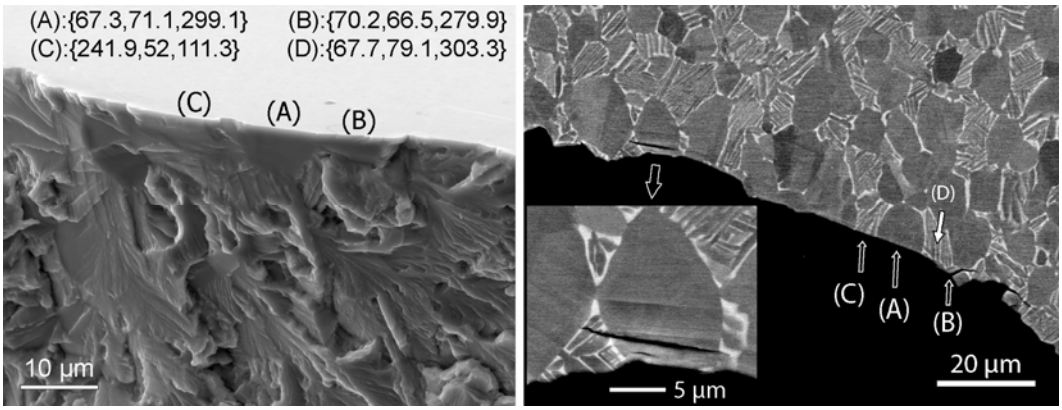

Figure 4. Crack initiation site and adjacent microstructure in the bi-modal condition. Max stress: 771 MPa, N_f = 54,403.

shown that the facets do not form as the result of a normal stress controlled cleavage mechanism in a single load stroke, but rather the crack tip advances incrementally through the grain over many cycles at low applied ΔK [10]. Low ΔK faceted growth is accompanied by the formation of steps [5,10], which are similar to river markings, and frequently occurs along the basal plane. These steps, which are generally parallel to one of the ‹a› directions, can be traced back to find the most probable crack initiation site.

3.1 Equiaxed microstructure

Crack initiation in the equiaxed condition occurred in primary α grains. One example is shown in Fig. 2 where three similar, but distinct, facets are labeled A, B and C. A fourth facet, D, which had increased surface roughness compared to the others, intersected the boundary between facets B and C. Facet A was more planar when imaged at high tilt angles while B and C had faint steps consistent with propagation by faceted growth [10]. Therefore, the most probable crack initiation scenario was that the crack started in grain A and propagated onto B, C and D by faceted growth. The normal of each of these facets made an angle of

25.3°, 28.3°, 35.9° and 51.8° with the loading direction, respectively. Because grain C was completely subsurface, diffraction patterns were obtained directly from the as-fractured facet to determine its orientation. The specimen was rotated after orientations A, B and D were determined, so, while sufficient to determine orientation of the c-axis with respect to the loading direction and the fracture plane (Fig. 3a), the Euler angles for C are unrelated to the prescribed sample reference frame and are not reported. Accounting for the spatial orientation of the individual facets verified that A, B and C were coincident with the basal plane while D was parallel to the first order pyramidal $\{10\bar{1}1\}$ plane (Fig. 3a).

The boundary between grains B and D also designates the boundary between two microtextured regions. Grains A, B and C belong to one region which have their c axes pointed towards the loading direction but are tilted 25° to 45°, having both high resolved shear and normal stresses on the basal plane. On the other side of the boundary, the grains in the microtextured region containing D have c-axes nearly perpendicular to the loading direction and are considered to be in an elastically and plastically 'softer' orientation [3]. A strain gradient must develop at the boundary to accommodate the different elastic responses of the microtextured regions. The local stress state appears to be favorable for crack initiation; however, the exact mechanism is not yet understood. As mentioned, these boundaries have already been implicated in dwell fatigue failure in Ti-6242 [2,3], however Ti-6-4 is not dwell sensitive [1] so the mechanisms are probably different.

3.2 Bi-modal microstructure

Despite the similar slip lengths in the equiaxed grains and α colonies, the cracks initiated consistently within primary α grains, but short crack propagation by faceted growth occurred through both α grains and α colonies. Elemental partitioning during α + β processing [1,6] results in a higher concentration of Al in the equiaxed α as compared to lamellar α. This causes increased slip planarity and preferential crack nucleation in the primary α grains. In contrast to the equiaxed material, no microtexture boundaries were observed within 100 μm of the crack initiation. In the example shown in Fig. 4, initiation occurred within grain (A) that was bordered by two transformed β colonies (C and D) (Fig. 4). While difficult to see in the backscattered image (Fig. 4), EBSD revealed that a constant orientation (B) extended almost to grain (A), in front of colony (D) which consequently did not directly border the fracture surface. The facet normal directions for (A) and (B) make angles of 23.8° and 32.7°, respectively, with the loading direction and were also within 5° of the basal pole (Fig. 3a). Facet C had a normal 37.6° from the loading axis and had a fracture plane within ~ 6° of $\{10\bar{1}1\}$. In terms of available slip length, (A) and (B) had similar basal plane orientations, so it may have been possible for slip to transfer over morphological barriers as discussed by Bridier et al. [19]. This occurrence results in increased local slip length. The near coincidence of the (0001) plane in (A) with the $\{10\bar{1}1\}$ in the adjacent grain (C) may be significant. Williams and Blackburn

have noted that the intersection of $\{10\bar{1}1\}<11\bar{2}3>$ and $(0001)<11\bar{2}0>$ slip bands can lead to the formation of dislocations with *c*[0001] Burgers vectors [9] which could assist in crack nucleation at the grain boundary. This is where cracks have been observed to form experimentally in the present study; however, additional work is needed to confirm this mechanism.

3.3 Fully lamellar microstructure

Crack initiation occurred near a g.b. α triple point at the intersection of two slip bands operating in colonies 1 and 2 (Fig. 5). The normal vectors of facets 1 and 2 make angles of 34.6° and 47.9°, respectively, with the loading direction. The crack extended by faceted growth onto the adjacent colony 3 which had a normal 46.8° to the loading direction and was approximately 400 μm in diameter. Considering the grain orientations (Fig. 5) and spatial orientations, all of the facet planes were coincident with the basal planes in their respective colonies (Fig. 3b). There was approximately 60° between the basal poles in colonies 1 and 2, which is similar to the misorientation between grains A and C in the bi-modal case discussed previously, but the adjacent colony (2) fractured on (0001) not $\{10\bar{1}1\}$.

On the top polished surface, as shown in Fig. 5, basal slip bands were present in all of the colonies adjacent to g.b. α. No slip bands were observed within g.b.1 and only faint slip traces were observed in g.b.2. At this level of detail, the slip bands are unaffected by the presence of α/β interfaces, but they were generally terminated at colony boundaries. The crystallographic and morphological relationships between the α and β phases imposed by the Burgers orientation relationship [1] allow dislocations on both basal and prismatic slip systems to pass through the α/β interfaces by means of a decomposition reaction; the details have been addressed in the literature [20,21]. While the colony size is clearly the slip length limiting feature in fully lamellar microstructures, crack initiation occurred in region of colony 1 that was limited to ~ 60 μm emphasizing the importance of local microstructure on crack initiation. Wojcik et al. [5] have noted that both resolved shear stress *and* normal stress were required for crack initiation in lamellar microstructures of Ti-811, so to a first approximation, the higher resolved normal stress on colony 1 compared to its neighbors may have made it a more favorable site for crack initiation.

3.4 Bi-lamellar microstructure

The secondary α precipitates were successful in blocking basal slip bands from traversing entire colonies, however, basal slip bands were evident within individual α laths (Fig. 6). Wegmann et al. [22] have shown that this microstructure increased the fatigue life of Ti-6-4 and Ti-6242 under full reverse loading (R = – 1). However, in the present study where R > 0 no appreciable difference in fatigue life was observed compared to the as-cast material. In fact, the majority of the data points fell within the same scatter band.

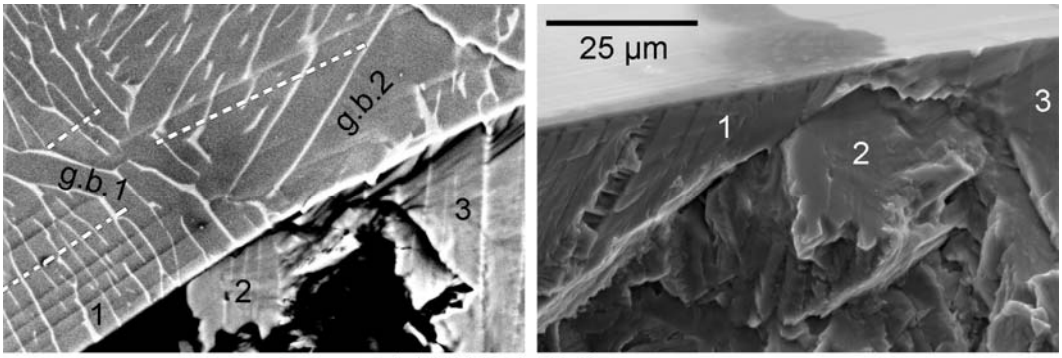

Figure 5. The microstructure and adjacent fracture surface of the fully lamellar sample. The traces of the basal planes are noted by the dotted white lines. Max stress: 750 MPa, N_f = 280,812.

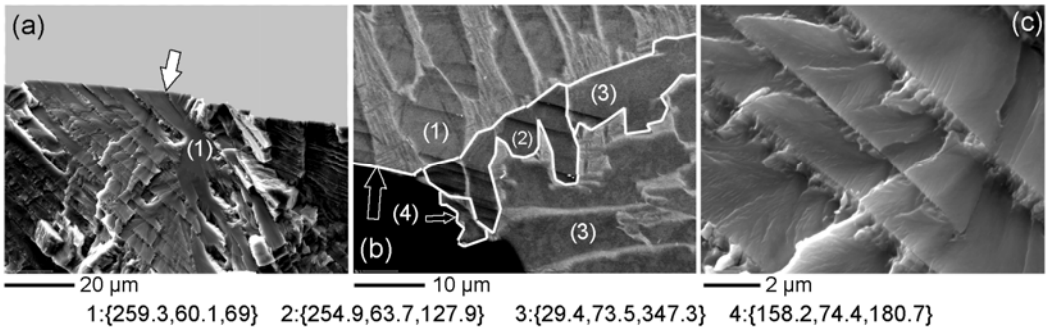

Figure 6. (a) The microstructure and (b,c) fracture surface of the bi-lamellar condition. Max stress: 750 MPa, N_f = 177,382. As a reference point, the arrow in (a) and (b) designates a common location in both images.

Crack initiation occurred within an α lath that was adjacent to g.b. α (Fig. 6). The face plane was coincident with the basal plane in colony (1) (Fig. 3b), which was inclined 33° relative to the loading axis. When no transformed β separated the α constituents, slip bands traversed the α/α boundaries despite the crystallographic and morphological differences. This resulted in an increase in local slip length at the grain boundary compared to in the colony. In this location, grain boundary α actually alternated its crystallographic orientation from (2) to (3), which were Burgers related by a 60° rotation about a common $<2\bar{1}\bar{1}0>$ axis. Two types of slip transfer were observed: from (1) → (2) and from (2) → (3). Colonies (1) and (2) are related by a 10.5° rotation about a common [0001] axis so a basal slip band can easily traverse this boundary. The second type of slip transfer occurred from the (0001) plane in colony (2) to a $\{10\bar{1}1\}$ plane in (3). While g.b. α and the adjacent colony (3) shared a common orientation, $\{10\bar{1}1\}$ slip bands were only observed in the grain boundary when there was an adjacent basal slip band active in colony (1). While no slip bands were observed to cross the from (1) to (4), it is interesting to note that one of the $\{10\bar{1}0\}$ planes in (4) was parallel to the basal plane in colony (1). Colony (4) was in an elastically 'softer' orientation compared to its neighboring colonies, being related to (1) by a 90° rotation about a common

$<2\bar{1}\bar{1}0>$ direction resulting in orthogonal c-axes. The elastic stresses that accommodate this abrupt orientation change, which are similar to the situation described in section 3.1, seem to be favorable for crack initiation.

For short FCG, Lutjering [6] has shown that FCG rates in bi-lamellar microstructures are reduced compared to fully lamellar. The reason for this is evident in Fig. 6c. Multiple variants of secondary α were precipitated in the β phase during the air cool which, as a consequence of the Burgers relation, have basal planes at 60^o or 90^o to each other. Since faceted growth occurs along crystallographic planes, the α precipitates cause the crack front to deviate out of plane. This process forms new steps are each time the crack tip encounters the β lamellae which consumes more energy and decreases the driving force for crack extension. A similar crack tip deflection process by secondary α can be observed in the inset of Fig. 4.

4.0 Summary and conclusions

In the Ti-6-4 alloy, high cycle fatigue crack initiation has been observed to consistently occur along slip bands irrespective of microstructural condition. Crack initiation occurred in grains that had their basal poles inclined between 25^o 45^o to the loading axis. The facet size correlated well with the slip length of each microstructural condition, however, slip planarity and local crystallography were also important factors affecting crack initiation. In particular, intense slip bands or cracks were formed when the basal plane of one grain was coincident with the (0001), $\{10\bar{1}0\}$ or $\{10\bar{1}1\}$ plane of its neighbor. Cracks initiation was not observed at random high angle boundaries.

5.0 Acknowledgement

Support for this work by the Office of Naval Research under Contract No. N00014-06-1-0089 is gratefully acknowledged.

6.0 References

[1] G. Lutjering and J.C. Williams, Titanium, Springer-Verlag, Heidelberg, 2003.
[2] A.P. Woodfield, M.D. Gorman, R.R. Corderman, J.A. Sutliff, and B. Yamrom, Effect of Microstructure on Dwell Fatigue Behavior of Ti-6242, in: *Titanium '95: Science and Technology*, P.A. Blenkinsop, W.J. Evans, H.M. Flower (eds.), (1995) 1116-1124.
[3] V. Sinha, J.E. Spowart, M.J. Mills, J.C. Williams, Observations on the Faceted Initiation Site in the Dwell-Fatigue Tested Ti-6242 Alloy: Crystallographic Orientation and Size Effects, Met. Mater. Trans., 37A (2006) 1507-1518.
[4] J.C. Chesnutt, A.W. Thompson, J.C. Williams, Influence of Metallurgical Factors on the Fatigue Crack Growth Rate in Alpha-Beta Titanium Alloys, AFML-TR-78-68 Final Technical Report, Air Force Materials Lab, Wright Patterson Air Force Base (1978).

[5] C.C. Wojcik, K.S. Chan, D.A. Koss, Stage I Fatigue Crack Propagation in a Titanium Alloy, *Acta Metall.*, 36(5), (1988) 1261-1270.
[6] G. Lutjering, Influence of processing on microstructure and mechanical properties of titanium alloys, Mat. Sci. Eng., A243 (1998) 31-45.
[7] M. Peters, A. Gysler, G. Lutjering, Influence of microstructure on the fatigue behavior of Ti-6Al-4V, Proc. 4th Int. Conf. Ti (1980) 1777-1786.
[8] J.C. Williams, R.G. Baggerly, N.E. Paton, Deformation Behavior of HCP Ti-Al Alloy Single Crystals, Met. Mater. Trans. 33A (2002) 837-850.
[9] M.J. Blackburn and J.C. Williams. Strength, Deformation Modes and Fracture in Titanium-Aluminum Alloys, ASM Quart. Trans., 62, (1969) p. 398.
[10] A.L. Pilchak, A. Bhattacharjee, R.E.A. Williams, J.C. Williams, The effect of local microstructure and crystallography on fatigue crack initiation in Ti-6Al-4V, submitted to Met. Trans. A.
[11] A.L. Pilchak, A. Bhattacharjee, A.H. Rosenberger, J.C. Williams, Low ΔK faceted growth in titanium alloys, Int. J. Fatigue, (2008) *in press*, doi: 10.1016/j.ijfatigue.2008.03.036
[12] D. C. Slavik, J.A. Wert, R.P. Gangloff, Determining fracture facet crystallography using electron backscatter patterns and quantitative tilt fractography, J. Mat. Res., 8(10) (1993) 2482-2491.
[13] V. Sinha, M.J. Mills, J.C. Williams, Determination of crystallographic orientation of dwell-fatigue fracture facets in Ti-6242 alloy, J. Mat. Sci., 42(19) (2007) 8334-8341.
[14] H. J. Bunge, Texture Analysis in Materials Science – Mathematical Methods, London, Butterworth & Co., 1982.
[15] J.F. Nye, Physical Properties of Crystals: Their Representation by Tensors and Matrices, Oxford Univ. Press, New York, 1985.
[16] J.V. Bernier, J.-S. Park, A.L. Pilchak, M.G. Glavicic and M.P. Miller, Measuring Stress Distributions in Ti-6Al-4V Using Synchrotron X-Ray Diffraction, Met. Trans. A, *in press, available online:* doi:10.1007/s11661-008-9639-6 (2008).
[17] S. Suresh, Fatigue of Materials 2nd ed., Cambridge Univ. Press, Cambridge, UK, 1998.
[18] G. J. Baxter, W.M. Rainforth, L. Grabowski, TEM Observations of Fatigue Damage Accumulation at the Surface of the Near-α Titanium Alloy IMI 834, Acta Mater., 44(9) (1996) 3453-3463.
[19] F. Bridier, P. Villechaise, J. Mendez, Analysis of the different slip systems activated by tension in a α/β titanium alloy in relation with local crystallographic orientation, Acta Mater. 53 (2004) 555-567.
[20] S. Suri, G.B. Viswanathan, T. Neeraj, D.-H. Hou, M.J. Mills, Acta mater., 47(3) (1999) 1019-1034.
[21] M.F. Savage, J. Tatalovich, M.J. Mills, Anisotropy in the room-temperature deformation of α-β colonies in titanium alloys: role of the α-β interface. Philosophical Magazine, 84(11) 1127-1154.
[22] G. Wegmann, J. Albrecht, G. Lutjering, K.-D. Folkers, C. Liesner, Microstructure and Mechanical Properties of Titanium Castings, Z. Metallkd., 88(10) (1997) 764-773.